RNA (2001), *7*:71–84. Cambridge University Press. Printed in the USA.

Arrangement of the central pseudoknot region of 16S rRNA in the 30S ribosomal subunit determined by site-directed 4-thiouridine crosslinking

DALIA I. JUZUMIENE and PAUL WOLLENZIEN

Department of Biochemistry, North Carolina State University, Raleigh, North Carolina 27695-7622, USA

ABSTRACT

The 16S rRNA central pseudoknot region in the 30S ribosomal subunit has been investigated by photocrosslinking from 4-thiouridine (s^4U) located in the first 20 nt of the 16S rRNA. RNA fragments (nt 1–20) were made by in vitro transcription to incorporate s^4U at every uridine position or were made by chemical synthesis to incorporate s^4U into one of the uridine positions at +5, +14, +17, or +20. These were ligated to RNA containing nt 21–1542 of the 16S rRNA sequence and, after gel purification, the ligated RNA was reconstituted into 30S subunits. Long-range intramolecular crosslinks were produced by near-UV irradiation; these were separated by gel electrophoresis and analyzed by reverse transcription reactions. A number of crosslinks are made in each of the constructs, which must reflect the structural flexibility or conformational heterogeneity in this part of the 30S subunit. All of the constructs show crosslinking to the 559–562, 570–571, and 1080–1082 regions; however, other sites are crosslinked specifically from each s^4U position. The most distinctive crosslinking sites are: 341–343 and 911–917 for $s^4U(+5)$; 903–904 (very strong), 1390–1397, and 1492 for $s^4U(+14)$; and 903–904 (moderate) for $s^4U(+17)$; in the 1070–1170 region in which there are different patterns for each s^4U position. These results indicate that part of the central pseudoknot is in close contact with the decoding region, with helix 27 in the 885–912 interval and with part of domain III RNA. Crosslinking between $s^4U(+14)$ and 1395–1397 is consistent with base pairing at U14-A1398.

Keywords: 16S rRNA three-dimensional structure; intramolecular RNA–RNA crosslinks; mRNA decoding region

INTRODUCTION

A feature of the 16S rRNA secondary structure first included in 1985 is the central pseudoknot interaction involving residues 17–19 and 916–918 (Pleij et al., 1985). These base pairs connect nucleotides in the loop of the first stem-loop structure and nt 916–918 that connect the second and third major RNA domains. The covariance of all three of these base pairs has now been established (Gutell, 1994).

The central pseudoknot is located in the middle part of the small ribosomal subunit. It has not been identified yet in the first X-ray structure descriptions of the 30S ribosomal subunit (Cate et al., 1999; Clemons et al., 1999; Tocilj et al., 1999); however, its position can be inferred because of the connections it has with the surrounding RNA segments that are known from the X-ray structures or are known from protein interactions and the locations of the proteins in the structure. Helix H27 (in the nucleotide interval 885–912) has been identified in the middle of the subunit structure with its beginning end closer to the cytoplasmic side of the 30S subunit and its end loop on the interface side of the 30S subunit (Cate et al., 1999; Clemons et al., 1999). Protein S4, which interacts with nucleotides in the 500–560 interval (Stern et al., 1989; Powers & Noller, 1995), and protein S5, which interacts with nucleotides in the 560 region, 910 region, and central pseudoknot region (Stern et al., 1989; Powers & Noller, 1995; Culver et al., 1999) are close to the central pseudoknot structure on the left side of the subunit body when the subunit is viewed from the interface side. Both proteins have been identified precisely in the X-ray structures (Clemons et al., 1999; Tocilj et al., 1999). Proteins S8, S15, S6, and S18, which interact with nucleotides in the middle RNA domain (Stern et al., 1989; Powers & Noller, 1995;

Reprint requests to: Paul Wollenzien, Department of Biochemistry, Box 7622, North Carolina State University, Raleigh, North Carolina 27695-7622, USA; e-mail: wollenz@bchserver.bch.ncsu.edu.

Lancaster et al., 2000), are located on the right side of the subunit body (Clemons et al., 1999; Lancaster et al., 2000).

The functional importance of the central pseudoknot has been investigated by mutational analysis. Brink et al. (1993) mutated C18 to A, G, or U and observed inhibition of in vivo translation activity. The mutant 30S subunits were not able to form 70S ribosomal complexes or polysomes, so a defect in translation initiation was suspected (Brink et al., 1993). Pinard et al. (1993, 1994, 1995) investigated mutations U13A (at the end of helix 1) and A914U adjacent to the central pseudoknot and observed effects in cell growth in vivo. In in vitro experiments, those mutations affected formation of the initiation complex but did not affect elongation activity (Pinard et al., 1995). Poot et al. (1996, 1998) substituted noncomplementary nucleotides to disrupt each of the three base pairs in the structure and found strongly impaired translational activity in all cases; restoration of base pairing with compensating mutations restored normal function. The functional defect in the subunits with the disrupted central pseudoknot base pairs was thought to be in subunit instability, because those subunits were deficient in proteins S1, S2, S18, and S21 (Poot et al., 1998). In addition, some of the double (compensating) substitutions should increase the stability of the (17–19)•(916–918) interaction (Poot et al., 1998) and these were normally functional. A proposal for the presence of alternate secondary structures involving the central pseudoknot was put forward to account for chemical reactivity changes seen upon the binding of streptomycin and to account for mutations in the 16S rRNA that induce streptomycin resistance (LeClerc & Brakier-Gingras, 1991; LeClerc et al., 1991). Another interaction between nt 14–17 and nt 1530–1534 was proposed to account for a conformational switch in the small subunit (Kossel et al., 1990). Poot et al. (1998) argued that some compensating mutations at (17–19)•(916–918) should provide stronger base pairing than the wild-type pairing and, because these did not affect ribosome function, this indicated that the central pseudoknot structure functions as a permanent structural element in the subunit.

The connection between the central pseudoknot and other parts of the ribosomal RNA was investigated in this study. RNA was prepared in which s^4U was substituted for uridine at different positions in the first 20 nt of the 16S rRNA. 30S subunits containing this RNA were irradiated with wavelengths that specifically activate s^4U for crosslinking. Intramolecular 16S rRNA crosslinks were identified and isolated by gel electrophoresis followed by reverse transcription analysis of crosslinking sites. The crosslinking sites include seven regions of the 16S rRNA that must be in the vicinity of the central pseudoknot. A large number of crosslinks are made by the s^4U substitutions, indicating that the region may be subject to significant conformational dynamics or structural heterogeneity in the isolated 30S subunits.

RESULTS

Synthesis and reconstitution of 16S rRNA with 4-thiouridine

4-thiouridine (s^4U) was incorporated into RNA containing the first 20 nt of the 16S rRNA sequence during in vitro transcription or chemical synthesis. In the first instance, in vitro transcription with T7 RNA polymerase was used to substitute all uridine positions with s^4U. This RNA, which had a 5-nt 5′ extension to the wild-type 5′ terminus, has s^4U substitutions at positions 5, 12, 13, 14, 17, and 20 and will be referred to as $s^4U(5–20)$. In the second instance, specific substitution of s^4U at positions +5, +14, +17, and +20 was accomplished during chemical synthesis of 20-nt fragments containing the wild-type 5′ terminus and sequence. Following gel purification, the 20- (or 25-) nt fragments and RNA fragments containing the sequence 21–1542 of the 16S rRNA, made by in vitro transcription, were mixed and annealed either with a 40-nt DNA that spanned the 20–21 junction or with a single strand DNA containing a sequence complementary to the 16S rRNA sequence (Fig. 1). Ligation was accomplished with T4 DNA ligase and following (RNase free) DNase I treatment and denaturation, the ligated RNA was gel purified to remove small DNA fragments and unligated RNA fragment 1–20 from the mixture. Ligation efficiency was usually 40–70%.

Reconstitution of the ligated RNA was done with total protein from 30S subunits (TP30) according to procedures developed for the reconstitution of synthetic 16S rRNA (Krzyzosiak et al., 1987). 30S subunits were isolated on sucrose gradients and showed sedimentation profiles typical of 30S subunits reconstituted from synthetic 16S rRNA (Fig. 2). The usual yield of 30S subunits compared to the input ligated RNA was about 25–30%, similar to the reconstitution yield from synthetic 16S rRNA. Typically fractions 6–13 were taken for concentration and analysis. The crosslinking results, including the pattern and crosslinking yield, did not change if a narrower fraction selection was made (e.g., fractions 6–9). The RNA preparations may contain the unligated large fragment RNA (nt 21–1542). However, because the sucrose gradients were analyzed by ^{32}P attached to the 20- or 25-nt fragment, particles containing only nt 21–1542 would not be observed. Because the subsequent crosslinking depends entirely on the s^4U carried by the small 1–20-nt RNA, any particles containing only 21–1532 RNA would not affect the structural analysis. The extent of association of the [^{32}P]-labeled, s^4U-containing subunits to 50S subunits is about 10–20% (data not shown), similar to

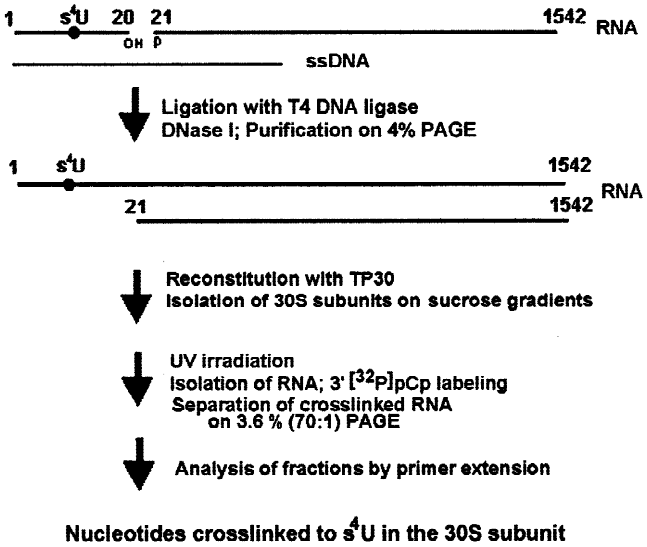

FIGURE 1. Scheme for the preparation and analysis of 16S rRNA with s^4U substitutions. s^4U was incorporated by reconstruction of the full-length 16S rRNA using an RNA fragment containing s^4U at a specific position. A DNA fragment was used to direct ligation by T4 DNA ligase (Moore & Sharp, 1992). For a small RNA fragment of 20 nt, a 40-nt DNA was used; for a small RNA fragment of 25 nt, a complete complementary single-stranded DNA (not indicated in the figure) was used and produced better ligation efficiency. Following DNase I treatment, unligated a small RNA fragment and DNA fragments were removed by electrophoresis on denaturing gels. The ligated large RNA is copurified with the unligated large RNA; however, in the subsequent irradiation experiment, only the ligated RNA was photoreactive by virtue of the s^4U located in the first 20 nt. Following reconstitution, 30S subunits were isolated and irradiated. RNA was isolated and the presence of crosslinks was determined by gel electrophoresis. The sites of crosslinking were determined by primer extension on the isolated crosslinked RNA.

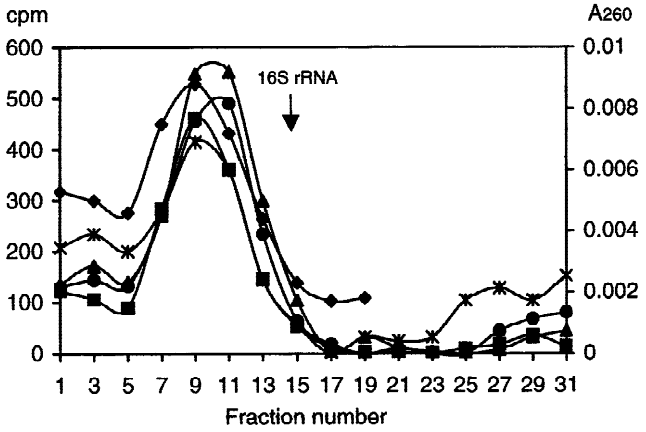

FIGURE 2. Sucrose gradient analysis of reconstituted 30S subunits. Ligated RNA was used in reconstitution experiments with TP30 following the reconstitution protocol of Krzyzosiak et al. (1987). The reconstitution mixes were centrifuged through linear 10–30% sucrose gradients in 1× RB buffer. A profile of particles reconstituted with synthetic 16S rRNA (♦-♦) from the A_{260} measurement of one twentieth of each fraction in the gradient is included for comparison. Profiles of particles reconstituted with $s^4U(+5)$ (●-●), $s^4U(+14)$ (▲-▲), $s^4U(+17)$ (■-■), and $s^4U(+20)$ (∗-∗) determined from radioactivity of each fraction are shown. A background measurement of the absorbance in the gradient and CPM from a blank sample have been subtracted from the A260 and radioactivity values. Centrifugation was right to left; the arrow shows the position of 16S rRNA.

30S subunits made with annealed RNA (Newcomb & Noller, 1999) and with synthetic RNA containing nt 1–1542 (Juzumiene & Wollenzien, 2000).

Analysis of crosslinks made by s^4U at different 16S rRNA sites

Reconstituted subunits were irradiated with UV light (320–380 nm) and RNA was isolated and ^{32}P labeled. Electrophoresis of the RNA on denaturing polyacrylamide gels demonstrates the presence of intramolecular crosslink, as linear 16S rRNA has a relatively fast mobility and covalent intramolecular crosslinks confer a reduced mobility. No crosslink were detected in samples containing s^4U that were not irradiated or in samples that were irradiated with the light source that was used, but did not contain s^4U (results not shown). Each of the five samples produced distinctive and reproducible patterns of crosslinking (Fig. 3). There were two common bands in the crosslink pattern for all of the samples. The first was the band numbered 1 (or 2 in samples $s^4U(+5)$ and $s^4U(+20)$); the second was the band numbered 8 (in sample $s^4U(+5)$, 6 (in samples $s^4U(+14)$, $s^4U(+17)$, and $s^4U(+20)$), and 7 (in sample $s^4U(5–20)$). Different patterns and band intensities occur at intermediate positions in each sample between these common bands.

Each lane in the preparative gel electrophoresis experiment was loaded with 30 μg RNA so the relative crosslinking can be judged by inspection of the gels. RNA from each of the most prominent bands in each sample was isolated by ultracentrifugation of the RNA out of the gel slices through CsCl cushions. RNA from each fraction was dissolved in an equal volume (except for RNA from the linear band of each sample, which was dissolved in a ten times larger volume). Therefore in subsequent primer extension experiments, the strength of the stops should indicate the relative frequency of crosslinking at each site.

Reverse transcription analysis of crosslinked RNA

Analysis by primer extension was carried out on RNA from all fractions to determine sites of crosslinking. Sites were identified visually by the intensity of bands specific to RNA from a particular fraction that do not appear in control lanes. In many instances there are a series of sites that are targets for crosslinking in particular regions (e.g., see the interval 559–562 in Fig. 4). In these instances, to make a judgment about which sites to list as crosslinks, band intensities were measured and positions that had a band intensity at

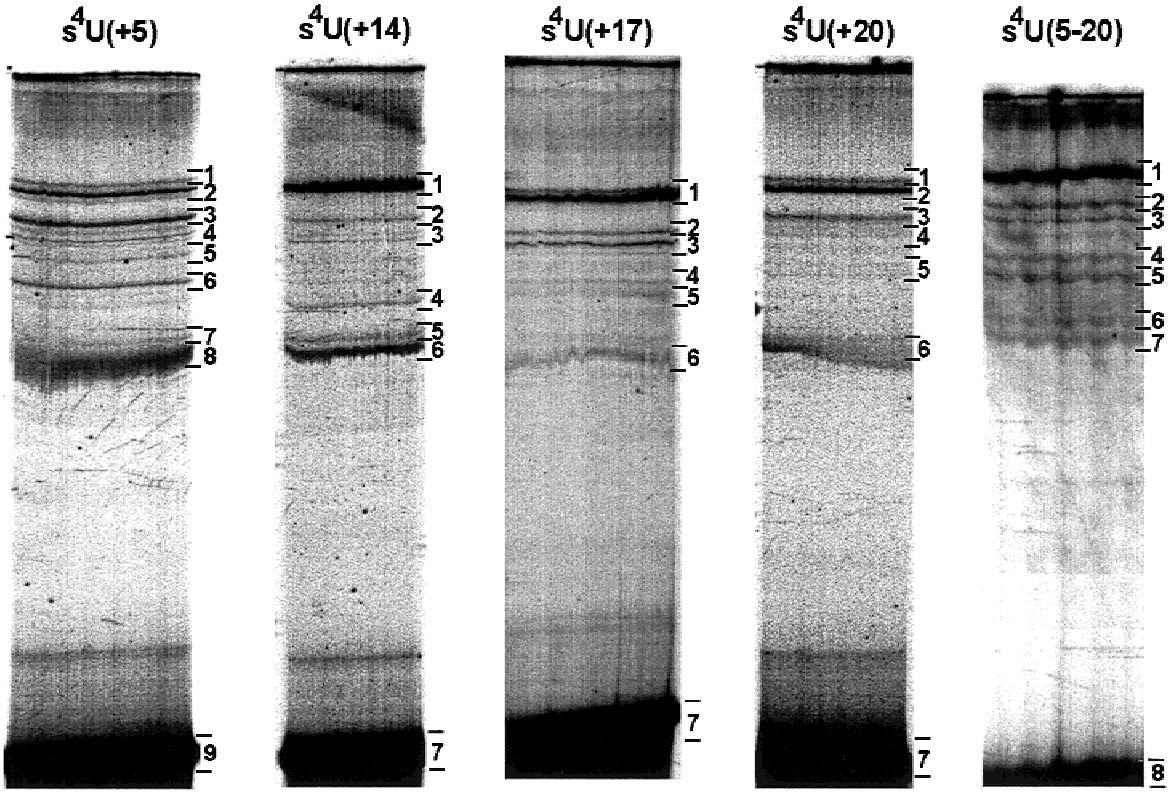

FIGURE 3. Gel electrophoresis analysis of RNA–RNA crosslinking by s^4U at different locations in the 16S rRNA. Crosslinked RNA was electrophoresed on 3.6% polyacrylamide gels (70:1; acrylamide:bis-acrylamide) in BTBE buffer (30 mM Bis-tris HCl, 30 mM boric acid, 2.5 mM EDTA, pH 6.8), 8.3 M urea at 45 °C for 18 h at 10 W. Each sample is identified by the position of the s^4U in the sequence. The positions of the excised bands are shown in the margin of each gel. Approximately 30 μg RNA were loaded on each lane. The bottom band (cut off in some lanes) has the mobility of uncrosslinked linear 16S rRNA.

least 50% greater than the corresponding band in the control lane (after normalization for the amount of RNA in each lane) were listed. Crosslinking sites in each case are taken as the nucleotide on the 5′ side of the reverse transcription stop sites (Lemaigre-Debreuil et al., 1991). In addition, there are natural stops in the reverse transcription samples that arise at sites where reverse transcriptase has paused and these were used to verify and normalize the amount of RNA from each sample. Thus, the crosslinking frequency at each site in the RNA could be specified semiquantitatively as +/−, +, and ++ to indicate marginal, moderate or strong crosslinking.

Crosslinks were detected in seven regions of the 16S rRNA. Reverse transcription showed these are for the regions around nt 340, 560–570, 910 (Fig. 4), 1080, 1120–1170 (Fig. 5), and 1400 and 1490 (Fig. 6). Altogether it was possible to account for crosslinks in all of the bands identified in Figure 3, except for the lowest of the common crosslinked bands in each sample (band 8 in sample $s^4U(+5)$, band 6 in samples $s^4U(+14)$, $s^4U(+17)$, and $s^4U(+20)$, and band 7 in sample $s^4U(5–20)$). This crosslink could result from crosslinking to a site in the extreme 3′ end of the 16S rRNA, but efforts to confirm this by an RNase H experiment were not successful.

Table 1 summarizes the location and relative intensity of the crosslinks in the 16S rRNA regions made by each s^4U construct. The sites of crosslinking in each construct are indicated in 16S rRNA secondary structure diagrams in Figure 7.

DISCUSSION

4-Thiouridine was substituted into positions U5 to U20 in the 16S rRNA by reconstructing full-length 16S rRNA by ligation, using fragments containing residues 1–20 and 21–1542. The s^4U placement sites are all in the vicinity of the central pseudoknot in the 16S rRNA secondary structure and they should be good monitors for the conformation of the central part of the 30S ribosomal subunit. The ligated RNAs could be reconstituted with ribosomal proteins using protocols developed for reconstitution of synthetic RNA (Krzyzosiak et al., 1987) and they form subunits with sedimentation profiles typical of synthetic 30S subunits. It has not been possible to characterize the functional properties of these subunits because of the small amount of mate-

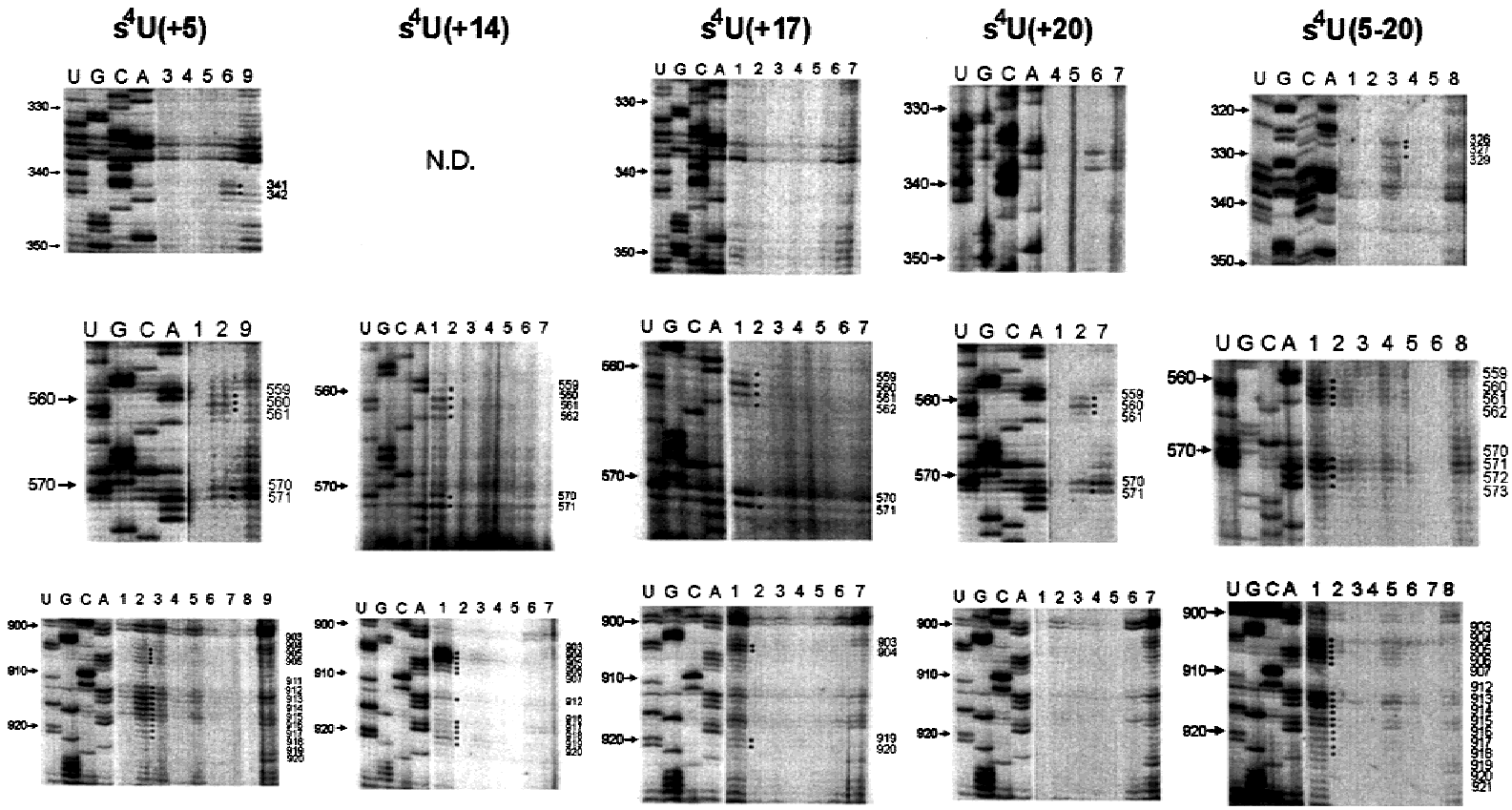

FIGURE 4. Reverse transcription analysis of crosslinking in the 340, 560–570, and 900–920 regions of the 16S RNA. Reverse transcription was done with primers for the indicated regions on fractions or selected fractions from each of the samples. The location of primer extension stopping sites first were determined visually; these were subsequently confirmed by intensity measurements, and bands that were at least 50% greater in intensity than the corresponding band in control lanes are marked in the gel. The sites of crosslinking (1 nt in the 5′ direction from the stopping site) are listed on the right margin. Positions at 10-nt intervals, read from the sequencing lanes, are shown in the left margin. Reverse transcription in the 330–350 region was not done on any fractions from the $s^4U(+14)$ sample in this experiment.

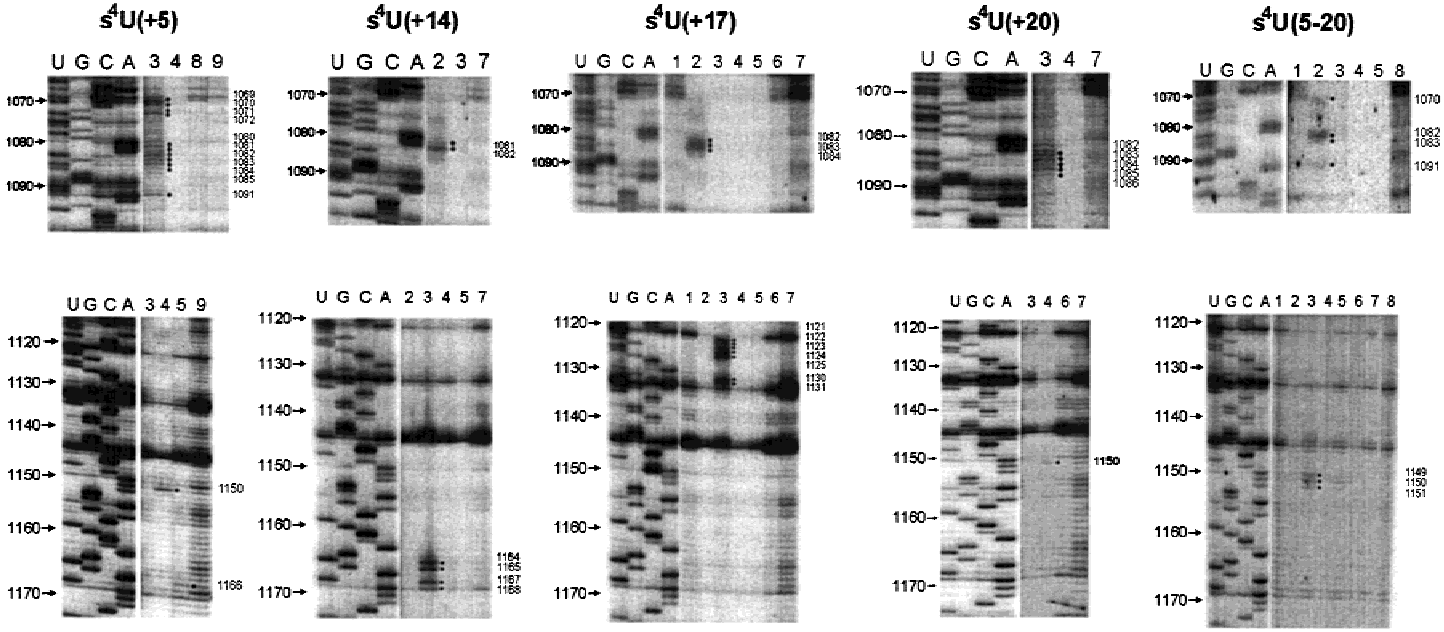

FIGURE 5. Reverse transcription analysis of crosslinking in the 1070–1090 and 1120–1170 regions of the 16S RNA. Reverse transcription was done with primers for the indicated regions on selected fractions from each crosslinked sample. The location of primer extension stopping sites that first were determined visually and confirmed by intensity measurements are marked in the gel. The sites of crosslinking (1 nt in the 5′ direction from the stopping site) are listed on the right margin. Positions at 10-nt intervals are shown in the left margin.

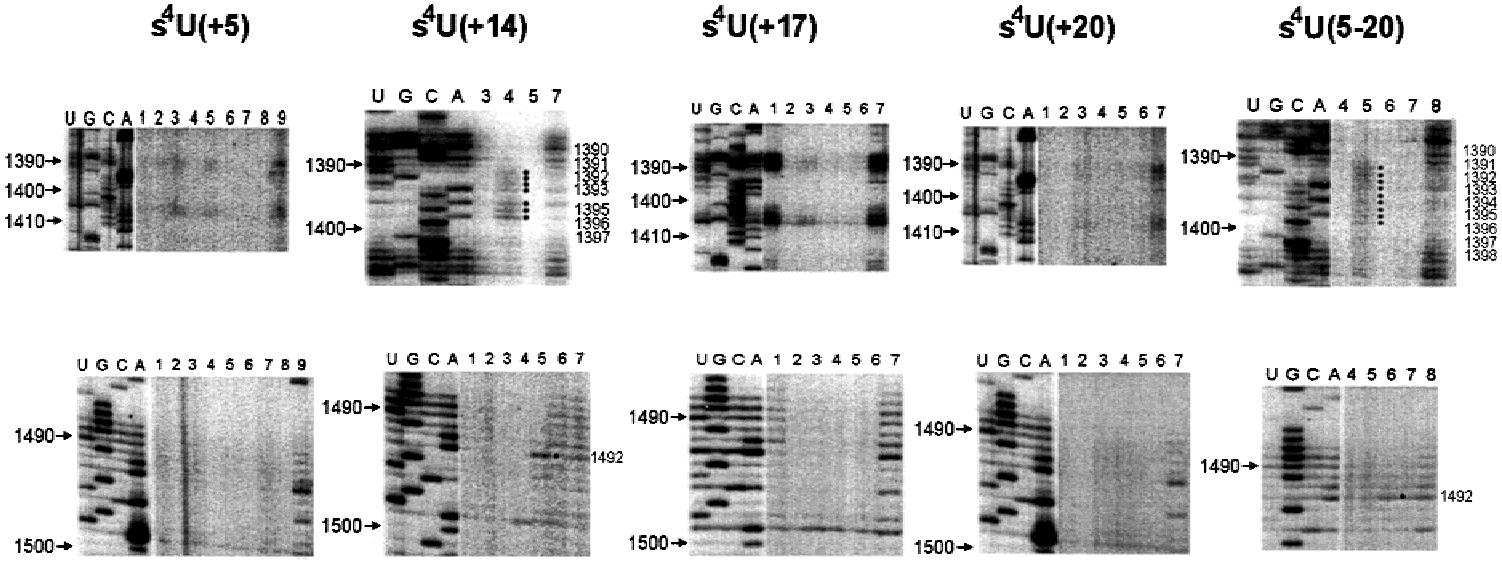

FIGURE 6. Reverse transcription analysis of crosslinking in the 1400 and 1492 regions of the 16S RNA. Reverse transcription was done with primers for the indicated regions on selected fractions from each crosslinked sample. The location of primer extension stopping sites that first were determined visually and confirmed by intensity measurements are marked in the gel. The sites of crosslinking (1 nt in the 5′ direction from the stopping site) are listed on the right margin. Positions at 10-nt intervals are shown in the left margin.

TABLE 1. Crosslinks by s^4U from positions 5–20 in 16S rRNA[a]

	s^4U position in the 16S rRNA				
Region in 16S rRNA	+5	+14	+17	+20	5–20
340	341–343+	N.D.[b]	—	—	326,327,329+
560–570	559–561+	559–562+	559–562+	559–561+	559–562+
	570–571+	570–571+	570–571+	570–571+	570–573+
900–920	903–906+/−	903–904++	903–904+		903–907++
	911–907+	905–907+/−		—	912–914++
	918–920+/−	912+/−	919–920+/−		915–921+/−
		916–920+/−			
1070–1090	1069–1070+				1070+/−
	1071–1072+				
	1080–1084+, 1085 +/−	1081–1082+	1082–1084+	1082–1085+	1082–1083+
	1091+/−			1086+/−	1091+/−
1120–1170	—	—	1121–1125+	—	—
			1130–1131+		
	1150+			1150+/−	1149–51+
		1164–1165++			
	1166+	1167–1168++			
1390	—	1390–1393+	—	—	1390–1398+
		1395–1397+			
1492	—	1492+	—	—	1492+/−

[a]Relative crosslink intensity judged from reverse transcription experiments is indicated by +/− (marginal), + (moderate), and ++ (strong).
[b]N.D.: not determined.

rials that are obtained. Synthetic 30S subunits have been described earlier as structurally similar to 30S subunits reconstituted with native 16S rRNA (Ericson et al., 1989, 1995; Moine et al., 1997; Juzumiene & Wollenzien, 2000) and having a partial reduction in functional activity compared to 30S subunits reconstituted with native 16S rRNA (Krzyzosiak et al., 1987; Denman et al., 1989; Cunningham et al., 1991). We cannot rule out that part of the 30S subunits contain misfolded 16S rRNA, but the profiles of the [^{32}P]- and s^4U-containing particles in the sucrose gradient indicate this is unlikely.

Irradiation with near-UV light produces RNA–RNA crosslinks in all of the reconstructions. Altogether, seven regions in all three major 16S rRNA domains contain sites of crosslinking. The list of crosslinks (Table 1) has been examined to separate the entries into general crosslinks seen for all s^4U positions and those seen only for specific positions (Table 2). Also only moderate and strong crosslinks have been retained in the list of Table 2. Three intervals are crosslinked by all of the s^4U substitutions. At the same time, the pattern of crosslinking is specific and informative because many other sites are crosslinked only by certain s^4U substitutions judged both by the pattern of bands seen in polyacrylamide gel electrophoresis and also because the pattern of reverse transcription stops is specific to each construct, even when bands of similar mobility are analyzed (see Figs. 3–7).

All of the sites determined by reverse transcription analysis were detected after gel electrophoresis purification of the slow mobility crosslinked products, so they cannot be due to artifacts from the irradiation process, such as base modification by energy transfer processes. Given that s^4U makes zero length crosslinks to covalently join nucleosides without any intervening linker, the patterns of crosslinking are not consistent with a single 30S conformation. Instead, the crosslink patterns must reflect the molecular flexibility or the conformational heterogeneity of the RNA in the 30S subunit in solution. Of the four positions that were specifically substituted, three positions (+5), (+14), and (+20) are not involved in base pairing in the secondary structure, so there may be greater conformational freedom in positioning of the uracil base in those instances. This pattern is reminiscent of the type of crosslinking specificity seen with s^4U crosslinking in a protein-free fragment of 16S rRNA (Lemaigre-Debreuil et al., 1991). It is surprising that the 30S subunit does not intrinsically limit the s^4U reactivity.

Three 16S rRNA intervals are crosslinked by all of the s^4U positions (Table 2, Fig. 8). The two intervals at 559–562 and 570–571 are part of the RNA strand that connects 16S rRNA domains I and II. This interval must be located behind the central pseudoknot if the 30S subunit is viewed from the interface side. The decoding region is on the interface surface (Cate et al., 1999; Clemons et al., 1999; Tocilj et al., 1999) and the central pseudoknot must be positioned immediately behind it to allow several interactions discussed in a following paragraph. By exclusion, this leaves the opposite side of the central pseudoknot for its encounter with the 559–562 and 570–571 intervals. The sites in the 1080–

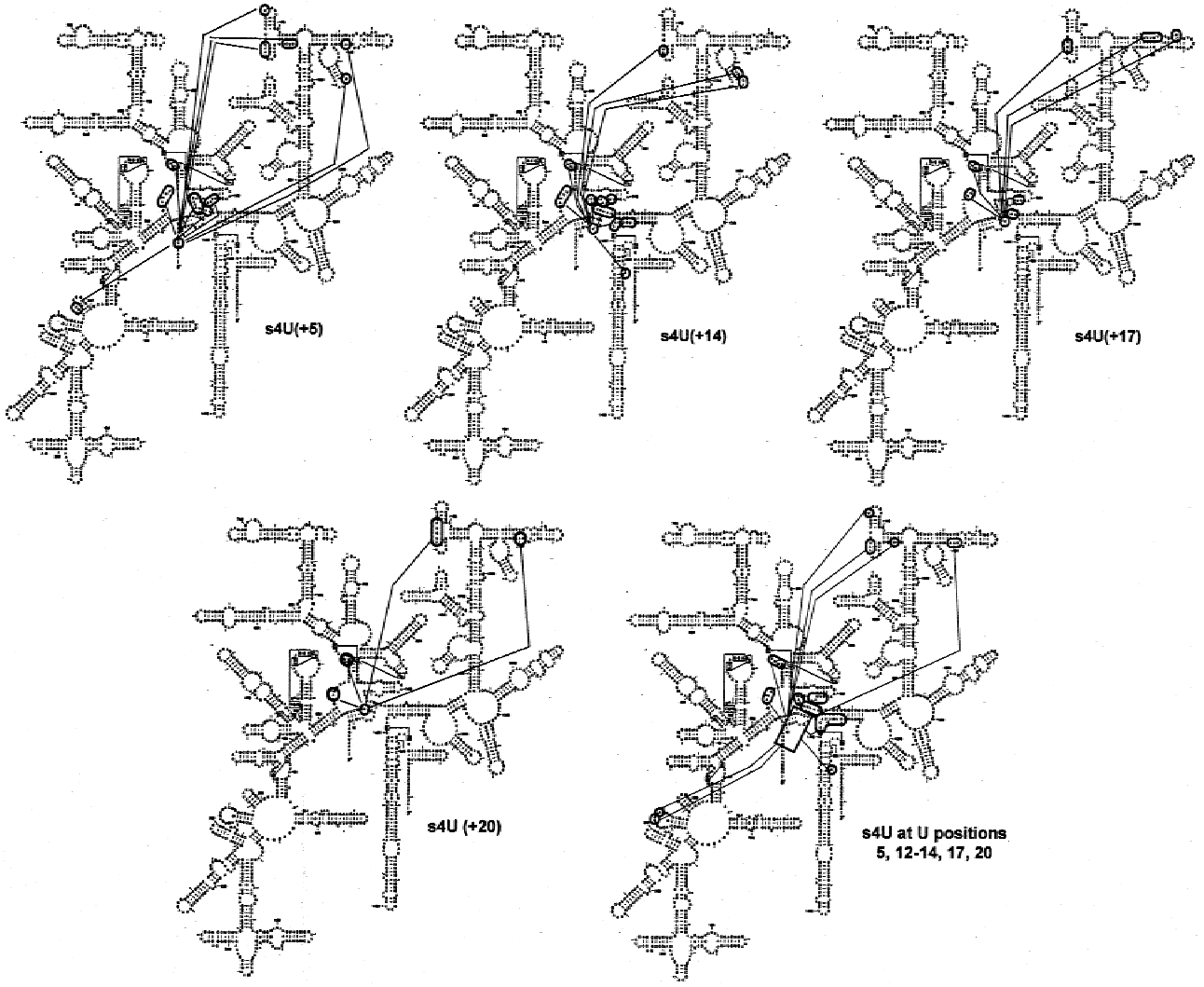

FIGURE 7. Summary of the crosslinks generated by s^4U from different positions in the neighborhood of the central pseudoknot. The five figures summarize results for s^4U substitution at (+5), (+14), (+17), (+20), and (5–20). All crosslinking sites are indicated here without regard to their relative strength. The *E. coli* 16S rRNA secondary structure diagram is from Gutell (1994).

1085 interval (and the other sites in domain III that are specifically crosslinked) are part of domain III and are associated with the RNA that is footprinted by ribosomal proteins S2 and S3 (Stern et al., 1989; Powers & Noller, 1995). These must be situated between the beak of the subunit head and the central pseudoknot located just below the very bottom of the head where it connects to the subunit body. Because all of these sites

TABLE 2. General and specific crosslinks from s^4U positions 5, 14, 17, and 20.[a]

		Specific crosslinks			
s^4U position	General crosslinks	340	903–12	Domain III	Decoding region
(+5)	559–561, 570–571, 1080–1084	341–343	911–917	1069–1070, 1150, 1166	
(+14)	559–562, 570–571, 1081–1082		903–904	1164–1165, 1167–1168	1390–1393,1395–1397, 1492
(+17)	559–562, 570–571, 1082–1084		904–904	1121–1125, 1130–1131	
(+20)	559–561, 570–571, 1082–1085				

[a]Crosslinks are listed as general if they were observed for all s^4U-substituted positions and are listed as specific if they were observed only from a subset of the substituted positions. Only crosslinks that were observed as moderate or strong are listed.

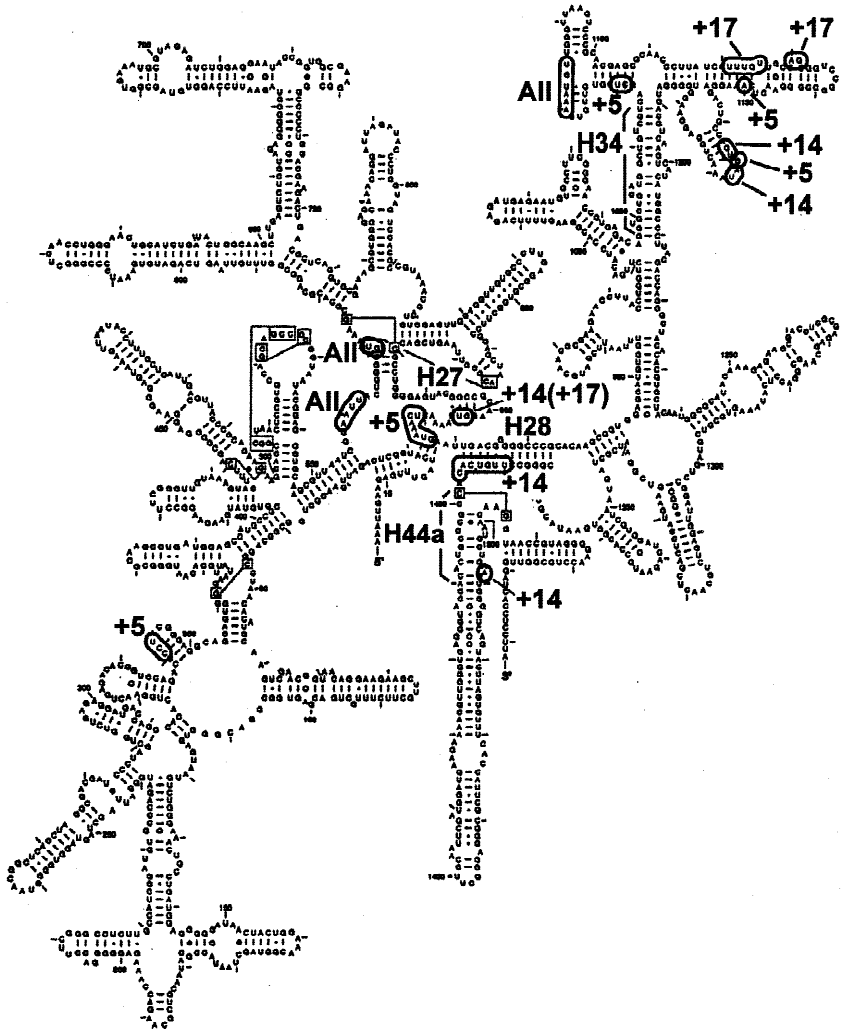

FIGURE 8. Summary of general and specific crosslinks. Three regions of general crosslinking indicated as "All" are shown in the 16S rRNA secondary structure within which all four of the s^4U substitutions have crosslinking sites. Positions specifically crosslinked with at least moderate frequency are marked by the s^4U position from which they are crosslinked. Helices H27, H28, H34, and H44a are indicated. The 16S rRNA secondary structure is from Gutell (1994).

are crosslinked by all four s^4U positions, it is impossible to make conclusions about the specific arrangement of the central pseudoknot with respect to these sites.

Four regions contain sites that are crosslinked by only one or two s^4U substitutions (Table 2, Fig. 8). The first is the 341–343 site (domain I) crosslinked only by $s^4U(+5)$. Other sites at 326–329 close to this interval are crosslinked by the $s^4U(5–20)$ construct (Table 1); these may come from the additional s^4U positions at 12 and 13 or because the $s^4U(5–20)$ construct has a slightly different arrangement due to the presence of additional 5′ nucleotides. Previously the distance from 343 to G9 was estimated as about 16 Å (Juzumiene & Wollenzien, 2000) and this is consistent with the present $s^4U(+5)$—341–343 crosslinks.

The second interval containing specifically crosslinked sites is in helix 27 (contained in the interval 885–912) and up to nt 917. The most prominent of the crosslinks here is the very strong $s^4U(+14)$ to 903–904. $s^4U(+17)$ crosslinks at a lower efficiency to 903–904. The pattern of $s^4U(+5)$ crosslinking in this interval is much different—it crosslinks in the interval 911–917, but very weakly to 903–904. Previously the G9 to 901 distance (60 Å) and G9 to 912 distance (up to 16 Å) had been estimated (Juzumiene & Wollenzien, 2000); the behavior of crosslinks from $s^4U(+5)$ and $s^4U(+14)$ are consistent with those estimates. These indicate that the central pseudoknot (particularly U(+14)) is closely associated with helix 27 and that the beginning of helix 1 (represented by G9 and U(+5)) is very far from nt 903–904 in the terminal base-paired part of helix H27.

The third RNA region with specific crosslinking sites is the S2/S3 subdomain of domain III. Each s^4U substitution crosslinks to sites in this part of domain III with at least moderate frequency (Table 2). These results suggest that the RNA fold of this part of domain III must somehow surround the 1080–1085 region and that this RNA subdomain is arranged in a specific way close to the central pseudoknot. These results are consistent with several other structural data pertaining to the overall domain III arrangement. A photocrosslink occurs in

synthetic domain III RNA between an azido reagent placed at G1193 and nucleotide A1394 (Montpetit et al., 1998) suggesting an arrangement of this part of domain III RNA to the bottom of helix 28, close to the central pseudoknot. RNA cleavage induced by an EDTA-FE(II) agent tethered to cysteine residue 21 on protein S5 occurred strongly in the central pseudoknot region and within helix H34, indicating their proximity (Culver et al., 1999). A base-triple interaction has been identified by comparative sequence analysis between base pair G933–C1384 and nucleotide C1109 (R.R. Gutell, S. Subashchandran, M. Schnare, Y. Du, N. Lin, L. Madabusi, K. Muller, N. Pande, N. Yu, Z. Shang, S. Date, D. Konings, V. Schweiker, B. Weiser, and J.J. Cannone, in prep.), which requires an arrangement in which C1109 interacts with the top of helix 28.

The fourth region with specific crosslinking sites is the decoding region. Two intervals at 1390–1397 (except 1394) and 1492 are crosslinked by $s^4U(+14)$. These two intervals must be in different positions. The 1390–1397 interval begins in helix H28 ((921–933)•(1384–1396)) and extends into helix H44a ((1399–1410)•(1490–1504)). The location of the decoding region has been identified in the crystal structures (Cate et al., 1999; Clemons et al., 1999; Tocilj et al., 1999) and in the cryoelectron microscopy images (Malhotra et al., 1998; Agrawal et al., 1999; Stark et al., 2000) because it is at the top of the visible penultimate long helix H44 and in the case of the functional complexes, the tRNA position indicates directly the site of the decoding region (Cate et al., 1999). The 1390–1397 interval must cross the neck of the subunit between the head and body. The 1492 site was identified in crystals containing tRNA (Cate et al., 1999); it is located in the back of H44a facing the body of the subunit. The central pseudoknot must be positioned so that U(+14) is close to 1390–1397, 1492, and helix H27 (particularly 903–904). This suggests that the base pairs (894-897)•(902-905) that contain 903 and 904 are close to A1492. This is consistent with the description that Cate et al. (1999) have given for the arrangement of A1492 and A1493. Clemons et al. (1999) described the location of the H27 helix in the 30S crystal structure as making a docking interaction with a minor groove of H44 close to the tRNA A site. However A1492/A1493 were not described in the structure, so it is not clear whether the docking seen in the crystal is consistent with the short distance suggested by the crosslinking of both A1492 and 903–904 to $s^4U(+14)$.

Some mitochondrial 16S rRNA sequences in the group Aves contain nucleotides at positions 14 and 1398 and at 15 and 1397 which covary with the predominant U-A and G-C identity, respectively (R.R. Gutell, S. Subashchandran, M. Schnare, Y. Du, N. Lin, L. Madabusi, K. Muller, N. Pande, N. Yu, Z. Shang, S. Date, D. Konings, V. Schweiker, B. Weiser, and J.J. Cannone, in prep.). However, there are single phylogenetic mutual changes underlying the covariations that are seen, so the significance of the covariation is uncertain. The $s^4U(+14)$ crosslinks to the 1390–1397 region indicate an arrangement in which U14 is close to this part of the decoding region. Possible base pairing of G15-C1397 and/or U14-A1398 were investigated by molecular modeling to determine if either or both of the interactions could be incorporated for the structure of the H44a, central pseudoknot, and H28 region (P. Babin, D.I. Juzumiene, M.A. Dolan, and P. Wollenzien, unpubl. observations). Molecular models could be made with a base pair involving G15 and C1397. These models helped to arrange the (17–19)•(916–918) interaction and the location and orientation of helix H28. These interactions would serve to help interlock the structure of the central part of the subunit and may be important in the function of the region.

There is a discrepancy in data concerning the function of nucleotides A1492 and A1493. These are implicated in tRNA binding at the A site by strong footprints that are seen with DMS modification (Moazed & Noller, 1986, 1990). Modification interference and mutagenesis experiments also identified A1492 and A1493 as important in A-site tRNA binding (Yoshizawa et al., 1999). Models have been proposed for the codon–anticodon interaction in the A site involving hydrogen bonding between A1492/A1493 and the ribose 2′ OHs of the mRNA at the A site (Yoshizawa et al., 1999) or between A1492/A1493 and the universally conserved U34 of the tRNA anticodon (VanLoock et al., 1999). In addition, mRNA photoaffinity labeling of the human 18S rRNA nucleotides corresponding to *Escherichia coli* nucleotides G1491 and A1492 has been reported from mRNA position (+4) in model complexes (Demeshkina et al., 2000) and mRNA photoaffinity labeling of *E. coli* A1492/A1493 has been detected with s^4U at position (+5) in an mRNA analogue (T. Shapkina & P. Wollenzien, unpubl. results). Two results indicate an arrangement different than this. The first was a description of contact between nucleotides A1492/A1493 and the body of the 30S subunit in the 70S ribosome X-ray structure (Cate et al., 1999). A1492/A1493 were described as facing away from the tRNA A site. It was suggested that changes in this contact upon subunit association or tRNA binding accounted for the chemical reactivity changes (Cate et al., 1999). The second is our observation of the $s^4U(+14)$ to A1492 crosslink that is consistent with a position for A1492 close to the subunit body rather than in the mRNA track. If A1492 is in the vicinity of helix H27, as described previously, it must face to the right side of the subunit rather than face the left side where the tRNA A site is located. The most likely way to account for these observations is in the possible conformational flexibility of the strand containing A1492. Because the location in the 30S subunit of the tRNA A site on the left of C1400 is well established (Agrawal et al., 1999, 2000; Cate et al., 1999), and it is

unlikely that there could be a large change in the position of the central pseudoknot without extensive unfolding of the center of the subunit, A1492 must have the capability to assume different positions. Some alternate configurations of helix 44a could be responsible for this and it is also possible that the conformational status of H27 participates in this change.

A scheme for translocation has been proposed that involves changes in the interactions between the RNA in the S4/530 region (in the interval 400–550) and the H34 region (in the interval (1047–1067)•(1189–1210) induced by EFG (Stark et al., 2000)). This was based on the structural changes seen in the 70S ribosome by cryoelectron microscopy. This change is proposed to affect the structure in the decoding region possibly mediated by protein S5 (Stark et al., 2000). The secondary structure conformational switch at the H27 region may also be involved in establishing a transition-state complex that allows movement of the mRNA/tRNA complex (Stark et al., 2000). The results presented here are relevant to part of the mechanics of this scheme. The present results suggest contacts between part of domain III 16S rRNA and the central pseudoknot, between the central pseudoknot and the decoding region, and between the central pseudoknot and helix H27. In addition, the results from molecular modeling investigations suggested a connection between the conformation of helix H28 and the spatial arrangement of the central pseudoknot (P. Babin, D.I. Juzumiene, M.A. Dolan, and P. Wollenzien, unpubl. observations). Thus several critical structure elements in the central part of the 30S subunit are connected by the central pseudoknot and may operate together in the ribosome.

MATERIALS AND METHODS

Preparation of RNA fragments

Small RNA fragments containing 16S rRNA sequence 1–20 were made by in vitro transcription (with complete s^4U substitution) or by chemical synthesis (with specific s^4U substitution). T7 RNA polymerase was used for the in vitro transcription using double-stranded DNA obtained by PCR. A 100-μL PCR reaction was done in standard PCR buffer with 1.5 mM $MgCl_2$, 0.2 mM each dNTP, 10 pmol single-stranded DNA template, and 100 pmol of left (containing T7 RNA promoter) and right primers. After denaturation for 5 min at 95 °C, 5 U *Taq* polymerase were added and 30 cycles of denaturation (30 s at 95 °C), annealing (30 s at 58 °C), and extension (30 s at 72 °C) steps were performed with final extension for 2 min at 72 °C. The reaction mix was phenol and ether extracted and passed through microcon-10 columns (Amicon) to separate the double-stranded PCR product from unincorporated primers and nucleotides.

To improve the in vitro transcription reaction, the DNA template had five extra nucleotides (GGAAA) added to the transcription start site and the uridine at position 4 was changed to cytidine. Standard 100-μL in vitro transcription reactions contained 50 pmol double stranded DNA; 40 mM Tris HCl, pH 7.5; 6 mM $MgCl_2$; 2 mM spermidine; 10 mM NaCl; 10 mM DTT; 1.25 mM each of ATP, CTP, and GTP; 0.25 mM s^4UTP; 100 U RNasin (Promega), 1 mM GMP, and 100 U T7 RNA polymerase. After 2 h incubation at 37 °C, DNase I (RNase free, Promega) was added and the reaction mix incubated for 30 min at 37 °C followed by phenol and ether extraction and ethanol precipitation. The transcript RNA was 5′ labeled by the exchange reaction using T4 polynucleotide kinase and [γ-^{32}P]-ATP and was purified on a 12% acrylamide:bisacrylamide (19:1)/urea/TBE gel. RNA from the gel was recovered by electroelution (Centrilutor, Amicon). The usual yield after the gel purification step was 25 μg of RNA from an initial 100 μL transcription reaction.

Four other 20-nt RNA fragments containing single s^4U substitutions were chemically synthesized with s^4U at positions 5, 14, 17, or 20 using commercial phosphoramidite reagents (Glen Research) and were deprotected using procedures supplied by the manufacturer. They were gel purified as described above.

The long RNA fragment containing the 21–1542 16S rRNA sequence was obtained by in vitro transcription from a plasmid containing an insert (obtained by PCR reaction). The plasmid was cut with a unique restriction site to produce run-off transcripts (Krzyzosiak et al., 1987). In vitro transcription was done using the Ribomax method in the presence of 12 mM GMP and 0.6 mM GTP. After 2 h incubation at 37 °C, additional T7 RNA polymerase was added and reaction mix was incubated for two more hours. Template DNA was digested with DNase I (RNase free, Promega) and reaction mix was phenol and ether extracted, passed through centricon-100 columns (Amicon) and ethanol precipitated. The usual yield from a 500-μL reaction was 400 μg of RNA.

Preparation of full-length complementary single-stranded DNA

Full-length single-stranded DNA complementary to 16S rRNA sequence was used as a template for ligation of a fully s^4U-substituted 25-nt RNA fragment with the rest of 16S rRNA. For this, the 16S rRNA gene obtained from pK3535 plasmid by PCR was cloned into the pTZ19R plasmid (US Biochemicals) and was transformed into the *E. coli* strain CJ236 or 71/18 that has *F′* episome. Under infection with helper phage M13K07, single-stranded DNA was produced that was complementary to the 16S rRNA sequence. Ligation reactions involving the chemiocall-synthesized 20-nt RNA fragment with the 21–1542 RNA fragment used a short single-stranded DNA oligonucleotide (40 nt) spanning the ligation site (Moore & Sharp, 1992).

T4 DNA ligase purification

T4 DNA ligase was purified from *E. coli* 594 strain lysogenized with the phage NM989 λT4lig *Wam*403 *cI*857 *nin*5 *Sam*100 (Murray et al., 1979) kindly provided by Dr. N. Murray, University of Edinburgh, Scotland. Purification was done according to the procedure of Tait et al. (1980) except for introduction of additional TSK-Gel Toyopearl DEAE-650 (Supelco) column to remove residual RNase activity. The usual

yield from 50 g cells was about 50 mg of T4 DNA ligase (about 70,000 U).

Ligation of RNA fragments

Usually part of the small RNA fragment was [γ-^{32}P]-ATP labeled by a T4 Polynucleotide kinase reaction for further monitoring of ligation, gel purification, and reconstitution events. Ligation of two RNA fragments using single-stranded DNA as a template was done according to Moore and Sharp (1992). Preparative scale ligation reactions were done in 10 mL ligation buffer containing 50 mM Tris HCl, pH 7.5; 10 mM $MgCl_2$; 20 mM DTT; 1 mM ATP; 50 μg/mL BSA; 1,000 U of RNasin (Promega); 1,000 pmol of each RNA fragment, and 1,000 pmol of single-stranded DNA. The reaction mix was incubated for 2 min at 55 °C and slowly cooled to the ice temperature. Five thousand units of T4 DNA ligase were added to the reaction and incubation was continued overnight at room temperature. Template single-stranded DNA was digested with DNase I (RNase free, Promega, 5 U to 1 μg of DNA) for 1 h at 37 °C. The reaction mix was phenol/ether extracted, passed through centricon-100 columns (Amicon) and ethanol precipitated. Under these conditions the efficiency of ligation is about 50%. Ligated 16S rRNA was separated from unligated small RNA fragment and single-stranded DNA pieces by denaturating 4% acrylamide:bis-acrylamide (40:1), 8.3 M urea in BTBE buffer (30 mM bis-Tris HCl, pH 6.8; 30 mM boric acid; 2.5 mM EDTA) gel, that was run for 3 h at 40 W. Ligated 16S rRNA was detected on a phosphorimager (because [^{32}P]-labeled small RNA fragment was used), cut from the gel, and recovered by ultracentrifugation through 2 M CsCl, 0.2 M EDTA, pH 7.4, cushions for 12 h at 40K rpm (Wilms & Wollenzien, 1994). These gel conditions are not able to separate ligated 16S rRNA from unligated 21–1542 RNA fragment, which differs by just 20 nt, but the 21–1542 fragment does not interfere subsequently in the crosslinking, as it does not have a s^4U group. The yield of RNA after the gel purification step was usually about 50% or 250 μg of ligated 16S rRNA together with the unligated 21–1542 RNA fragment.

Reconstitution of 30S ribosomes

Reconstitution of 30S ribosomes was done according Krzyzosiak et al. (1987) with some changes. Two hundred micrograms of gel-purified RNA in 200 μL of 0.1× Rec-20 buffer (1× Rec-20 buffer is 20 mM HEPES, pH 7.5; 0.4 M NH_4Cl; 20 mM $Mg(OAc)_2$; 3 mM β-mercaptoethanol) were incubated for 5 min at 40 °C. This was brought to 1 mL reconstitution mix containing 1× Rec-20 buffer with 0.5 M NH_4Cl. After additional incubation for 5 min at 40 °C, TP30 ribosomal protein fraction was added (4× excess in equivalents) and reconstitution was performed for 10 min at 40 °C; 15 min at 43 °C; 15 min at 46 °C; 15 min at 48 °C with final incubation for 3 min at 50 °C. After short cooling on ice, samples were applied on the 10–30% linear sucrose gradients in 1× RB buffer (20 mM HEPES, pH 7.5, 0.1 M NH_4Cl, 10mM $Mg(OAc)_2$, 3 mM β-mercaptoethanol) and centrifuged for 18 h at 27K rpm. Fractions containing 30S (detected by radioactivity or A_{260} measurements) were pooled, sedimented by ultracentrifugation, dissolved in the activation buffer (20 mM Tris-HCl, pH 7.5; 200 mM NH_4Cl; 20 mM $MgCl_2$; 3 mM β-mercaptoethanol), and used for crosslinking. The usual yield of reconstituted 30S ribosomes was 30%.

Crosslinking

One hundred picomoles of reconstituted 30S in 500 μL activation buffer were activated for 20 min at 37 °C, cooled on ice, and irradiated at 10 °C with a mercury light irradiator (λ_{max} at 365 nm) that has the intensity of light (after filtration with $CoNO_3$ filter) of about 100 mW/cm^2. RNA was phenol and ether extracted from 30S ribosomes after 2% SDS, 20 mM EDTA, and 1 mg/mL proteinase K treatment for 30 min at 37 °C, and ethanol precipitated. Part of the RNA was 3′-end labeled with [^{32}P]-pCp and T4 RNA ligase (England & Uhlenbeck, 1978). Crosslinked RNA species were separated on a denaturing gel (3.6% acrylamide:bis-acrylamide (70:1), 8.3 M urea in BTBE buffer), that was run for 18 h at 10 W and 45 °C using a thermostatted gel apparatus. Crosslinked and uncrosslinked RNA was detected on a phosphorimager and extracted from the gel by ultracentrifugation through CsCl cushions using 40 μg of total tRNA (*Bacillus subtilis*) as a carrier. RNA pellets were dissolved in H_2O, phenol and ether extracted, ethanol precipitated, and used for reverse transcription analysis.

Reverse transcription analysis

Primer extension using AMV reverse transcriptase was used to determine 16S rRNA crosslinked nucleotides as described previously (Wollenzien, 1988). Seven DNA primers were used to read all or the 16S rRNA except for the 3′ terminal 20 nt. cDNA was electrophoresed on 8% acrylamide:bis-acrylamide (19:1), 8.3 M urea in TBE buffer (89 mM Tris base, 89 mM boric acid, 2 mM EDTA, pH 8.3) gels.

ACKNOWLEDGMENTS

This work was supported by a grant from the National Institutes of Health (GM43237). Dr. Noreen Murray is thanked for very kindly providing the *E. coli* strain producing T4 DNA ligase. We thank Tatjana Shapkina and Stanislav Kirillov for critical reading of the manuscript.

Received August 28, 2000; returned for revision September 27, 2000; revised manuscript received October 5, 2000

REFERENCES

Agrawal R, Penczek P, Grassucci R, Burkhardt N, Nierhaus K, Frank J. 1999. Effect of buffer conditions on the position of tRNA on the 70S ribosome as visualized by cryoelectron microscopy. *J Biol Chem 13*:8723–8729.

Agrawal R, Spahn C, Penczek P, Grassucci R, Nierhaus K, Frank J. 2000. Visualization of tRNA movements on the *Escherichia coli* 70S ribosome during the elongation cycle. *J Cell Biol 150*:447–459.

Brink M, Verbeet M, de Boer H. 1993. Formation of the central pseudoknot in 16S rRNA is essential for initiation of translation. *EMBO J 12*:3987–3996.

Cate JH, Yusupov MM, Yusupova GZ, Earnes TN, Noller HF. 1999. X-ray crystal structures of 70S ribosome functional complexes. *Science 285*:2095–2104.

Clemons WMJ, May JLC, Wimberly BT, McCutcheon JP, Capel MS, Ramakrishnan V. 1999. Structure of a bacterial 30S ribosomal subunit at 5.5 Angstroms resolution. *Nature 400*:833–840.

Culver GM, Heilek GM, Noller HF. 1999. Probing the rRNA environment of ribosomal protein S5 across the subunit interface and inside the 30S subunit using tethered Fe(II). *J Mol Biol 286*:355–364.

Cunningham P, Richard R, Weitzmann C, Nurse K, Ofengand J. 1991. The absence of modified nucleotides affects both in vitro assembly and in vitro function of the 30S ribosomal subunit of *Escherichia coli*. *Biochimie 73*:789–796.

Demeshkina N, Repkova M, Ven'yaminova A, Graifer D, Karpova G. 2000. Nucleotides of 18S rRNA surrounding mRNA codons at the human ribosomal A, P, and E sites, respectively: A crosslinking study with mRNA analogues carrying aryl azide group at either the uracil or the guanine residue. *RNA 6*:1727–1736.

Denman R, Negre D, Cunningham PR, Nurse K, Colgan J, Weitzmann C, Ofengand J. 1989. Effect of point mutations in the decoding site (C1400) region of 16S ribosomal RNA on the ability of ribosomes to carry out individual steps of protein synthesis. *Biochemistry 28*:1012–1019.

England T, Uhlenbeck O. 1978. 3′-terminal labeling of RNA with T4 RNA ligase. *Nature 275*:560–561.

Ericson G, Chevli K, Wollenzien P. 1989. Structure of synthetic unmethylated 16S ribosomal RNA as purified RNA and in reconstituted 30S ribosomal subunits. *Biochemistry 28*:6446–6454.

Ericson G, Minchew P, Wollenzien P. 1995. Structural changes in base-paired region 28 in 16S rRNA close to the decoding region of the 30S ribosomal subunit are correlated to changes in tRNA binding. *J Mol Biol 250*:407–419.

Gutell RR. 1994. Collection of small subunit (16S and 16S-like) ribosomal RNA structures: 1994. *Nucleic Acids Res 22*:3502–3507.

Juzumiene DI, Wollenzien P. 2000. Organization of the 16S rRNA around its 5′ terminus determined by photochemical crosslinking in the 30S ribosomal subunit. *RNA 6*:26–40.

Kossel H, Hoch B, Zeltz P. 1990. Alternative base pairing between the 5′- and 3′-terminal sequences of small subunit RNA may provide the basis of a conformational switch of the small ribosomal subunit. *Nucleic Acids Res 18*:4083–4088.

Krzyzosiak W, Denman R, Nurse K, Hellmann W, Boublik M, Gehrke CW, Agris PF, Ofengand J. 1987. In vitro synthesis of 16S ribosomal RNA containing single base changes and assembly into a functional 30S ribosome. *Biochemistry 26*:2353–2364.

Lancaster L, Culver GM, Yusupova GZ, Cate JH, Yusupov MM, Noller HF. 2000. The location of protein S8 and surrounding elements of 16S rRNA in the 70S ribosome from combined use of directed hydroxyl radical probing and X-ray crystallography. *RNA 6*:717–729.

LeClerc D, Brakier-Gingras L. 1991. A conformational switch involving the 915 region of *Escherichia coli* 16 S ribosomal RNA. *FEBS Lett 279*:171–174.

LeClerc D, Melancon P, Brakier-Gingras L. 1991. Mutations in the 915 region of *Escherichia coli* 16S ribosomal RNA reduce the binding of streptomycin to the ribosome. *Nucleic Acids Res 19*:3973–3977.

Lemaigre-Debreuil Y, Expert-Bezancon A, Favre A. 1991. Conformation and structural fluctuations of a 218 nucleotides long rRNA fragment: 4-thiouridine as an intrinsic photolabeling probe. *Nucleic Acids Res 19*:3653–3660.

Malhotra A, Penczek, Agrawal RK, Gabashivili IS, Nierhaus KH, Frank J. 1998. *Escherichia coli* 70S ribosome at 15 Å resolution by cryo-electron microscopy: Localization of fMet-tRNA$_f^{Met}$ and fitting of L1 protein. *J Mol Biol 203*:103–116.

Moazed D, Noller HF. 1986. Transfer RNA shields specific nucleotides in 16S ribosomal RNA from attack by chemical probes. *Cell 47*:985–994.

Moazed D, Noller HF. 1990. Binding of tRNA to the ribosomal A and P sites protects two distinct sets of nucleotides in 16S rRNA. *J Mol Biol 211*:135–145.

Moine H, Nurse K, Ehresmann B, Ehresmann C, Ofengand J. 1997. Conformational analysis of *Escherichia coli* 30S ribosomes containing the single-base mutations G530U, U1498G, G1401C, C1501G and the double-base mutation G1401C/C1501G. *Biochemistry 36*:13700–13709.

Montpetit A, Payant C, Nolan JM, Brakier-Gingras L. 1998. Analysis of the conformation of the 3′ major domain of *Escherichia coli* 16S ribosomal RNA using site-directed photoaffinity crosslinking. *RNA 4*:1455–1466.

Moore MJ, Sharp PA. 1992. Site specific modification of pre-mRNA: The 2′-hydroxyl groups at the splice sites. *Science 256*:992–997.

Murray N, Bruce S, Murray K. 1979. Molecular cloning of the DNA ligase gene from bacteriophage T4. *J Mol Biol 132*:493–505.

Newcomb L, Noller HF. 1999. Directed hydroxyl radical probing of 16S ribosomal RNA in 70S ribosomes from internal positions of the RNA. *Biochemistry 38*:945–951.

Pinard R, Cote M, Payant C, Brakier-Gingras L. 1994. Positions 13 and 914 in *Escherichia coli* 16S ribosomal RNA are involved in the control of translational accuracy. *Nucleic Acids Res 22*:619–624.

Pinard R, Payant C, Brakier-Gingras L. 1995. Mutations at positions 13 and/or 914 in *Escherichia coli* 16S ribosomal RNA interfere with the initiation of protein synthesis. *Biochemistry 34*:9611–9616.

Pinard R, Payant C, Melancon P, Brakier-Gingras L. 1993. The 5′ proximal helix of 16S rRNA is involved in the binding of streptomycin to the ribosome. *FASEB J 7*:173–176.

Pleij CWA, Rietfeld K, Bosch L. 1985. A new principle of RNA folding based on pseudoknotting. *Nucleic Acids Res 13*:1717–1731.

Poot RA, Pleij CWA, van Duin J. 1996. The central pseudoknot in 16S ribosomal RNA is needed for ribosome stability but is not essential for 30S initiation complex formation. *Nucleic Acids Res 24*:3670–3676.

Poot RA, van den Worm SH, Pleij CWA, van Duin J. 1998. Base complementarity in helix 2 of the central pseudoknot in 16S rRNA is essential for ribosome functioning. *Nucleic Acids Res 26*:549–553.

Powers T, Noller HF. 1995. Hydroxyl radical footprinting of ribosomal proteins on 16S rRNA. *RNA 1*:194–209.

Stark H, Rodnina MV, Wieden HJ, van Heel M, Wintermeyer W. 2000. Large-scale movement of elongation factor G and extensive conformational change of the ribosome during translocation. *Cell 100*:301–309.

Stern S, Powers T, Changchien L-M, Noller HF. 1989. RNA–protein interactions in 30S ribosomal subunits: Implications for folding and function of 16S rRNA. *Science 244*:783–790.

Tait R, Rodriquez R, West R Jr. 1980. The rapid purification of T4 DNA ligase from a lambdaT4 ligase lysogen. *J Biol Chem 255*:813–815.

Tocilj A, Schlunzen F, Janell D, Gluhmann M, Hansen HAS, Harms J, Bashan A, Bartels H, Agmon I, Franceschi F, Yonath A. 1999. The small ribosomal subunit from *Thermus thermophilus* at 4.5 Å resolution: Pattern fittings and the identification of a functional site. *Proc Natl Acad Sci USA 96*:14252–14257.

VanLoock MS, Easterwood TR, Harvey SC. 1999. Major groove binding of the tRNA/mRNA complex to the 16S ribosomal RNA decoding site. *J Mol Biol 285*:2069–2078.

Wilms C, Wollenzien P. 1994. Purification of RNA from polyacrylamide gels by ultracentrifugation. *Anal Biochem 221*:204–205.

Wollenzien P. 1988. Isolation and identification of RNA cross-links. *Methods Enzymol 164*:319–329.

Yoshizawa S, Fourmy D, Puglisi JD. 1999. Recognition of the codon–anticodon helix by ribosomal RNA. *Science 285*:1722–1725.